Theoretical Models and Experimental Analysis of Artificial Torsion Field and Gravitational Field Generated by the Vortex Electromagnetic Fields of Scalar Waves

Jiang Jian-zhong

School of Mechanical Engineering, Jiangnan University; Wuxi, 214122, China

Corresponding Author: Jiang Jian-zhong (Email: 8043000163@jiangnan.edu.cn)
(Received: 05-January-2026; accepted: 26-March-2026; published: 30-June-2026)
http://dx.doi.org/10.55579/jaec.2026102.532

Abstract. *Due to the absence of rigorous mathematical modeling and extensive experimental validation, the applications of torsion fields—such as zero-point energy extraction and therapeutic functionalities—remain in the hypothetical stage. Currently, the mainstream physics community has not recognized torsion field as a fundamental force, and research in this domain continues to reside within the realm of fringe science. Building upon the precise modeling of the vacuum scalar wave equations and particle propagation mode, we derived a theoretical framework for the generation of artificial torsion fields and gravitational field via vacuum scalar wave vortex electromagnetic fields, thereby elucidating the intrinsic correlation between these two field phenomena. Additionally, we conducted preliminary experiments to qualitatively verify the directional characteristics of artificial torsion and gravitational fields induced by vortex electromagnetic fields. Our study further provides profound insights into the fundamental nature of torsion and gravitational fields: the torsion field is an acceleration field associated with the tangential rotational motion of local space, whereas the gravitational field is an acceleration field corresponding to the radial curvilinear motion of local space.*

Keywords: *Quantum electrodynamics, torsion field, gravitational field, scalar wave, unified field equation.*

1. Introduction

Dr. Nikolai Kozyrev of the former Soviet Union put forward an important fundamental concept: The invariant of a particle is typically accompanied by a physical field. A particle with a fixed mass is accompanied by a gravitational field, one with a fixed charge is accompanied by an electromagnetic field. Therefore, a particle with a fixed spin should also be accompanied by a spin field, namely the torsion field [1]. Kozyrev further validated the anomalous interaction between rotating objects and spacetime via gyroscope experiments, thereby providing preliminary experimental clues for the existence of torsion fields [1]. Subsequently, through high-precision experimental observations, Hayasaka H detected the anomalous weight-reduction effect of rotating gyroscopes. This effect, which correlates with rotational speed and direction, cannot be accounted for by classical mechanics or general relativity, thus offering direct experi-

mental evidence in support of Kozyrev's torsion field hypothesis [2].

Given the extremely weak static intensity of the torsion field—approximately 10^{27} times weaker than gravitational force—Einstein temporarily neglected the effect of the torsion field when formulating general relativity, aiming to simplify theoretical derivations and focus on the influence of curvature on spacetime [3]. In 1920, Cartan [4] became the first to incorporate spacetime distortion effects induced by object spin within the framework of general relativity, laying the initial geometric foundation for the torsion field. Within Riemann–Cartan spacetime, the coupling of particle spin and orbital motion gives rise to the torsion field. While its static intensity remains extremely low, the intensity of the torsion field can be significantly enhanced under dynamic conditions—a property that provides a critical premise for subsequent experimental detection and application exploration of the torsion field. Russian physicist Gennady Shipov further advanced the mathematical theory of the torsion field, framing it as an extension and supplement to general relativity, which fills the gap in traditional gravitational theories that fail to account for spin effects [5].

As research advances, scholars worldwide have successively uncovered a range of distinctive properties and operational laws of torsion fields. Jiang X. L.'s studies demonstrate that torsion fields with vortex dynamic characteristics can interact with the zero-point vacuum energy field to form coherent (resonant) torsion field states. At the vortex center of the torsion field, high-energy rays, neutrons, and various high-energy particles are generated, while vacuum zero-point free energy can be harvested—often accompanied by highly directional cold nuclear fusion. This provides a novel paradigm for research on vacuum energy extraction and the controllability of cold nuclear fusion [6].

His key findings are concentrated in the exploration of vortex dynamics and anomalous nuclear phenomena: through electrochemical experiments, he validated the coherence mechanism between torsion fields (induced by the tip effect) and vacuum zero-point energy, with relevant conclusions having undergone repeated verification and gained attention from international peers [7]. Lee, S. C. investigated the physical properties of crystal torsion fields [8]; Jiang J. Z. theoretically demonstrated the correlation between scalar wave torsion fields and Qi in traditional Chinese medicine [9]; Don, R. clarified the excitation conditions, transmission pathways, and extraction mechanisms of vacuum energy during electromagnetic–torsion field coupling [10]. Meyl's research further revealed that torsion fields exhibit unique traits such as superluminal propagation, non-shielding, memory effects, energy-carrying capacity, and potential medical therapeutic functions. The memory effect allows torsion fields to retain spatial vortex structures even after the source field is removed, while non-shielding enables them to penetrate conductive media without attenuation [11]. Physically, torsion fields can be regarded as the transverse polarization of the physical vacuum under spin perturbation, together with electromagnetic fields and gravitational fields forming the three polarization states of the vacuum under distinct perturbation conditions [3].

Despite substantial progress in torsion field research, the mainstream physics community has not formally recognized torsion fields as a fifth fundamental force—owing to the lack of a rigorous, comprehensive mathematical model and the absence of repeatable, high-precision experimental validation methods. Related applications remain in the stage of theoretical hypothesis and exploration, and some research findings in this field have long been questioned by mainstream academia [12]. To date, over ten thousand relevant research papers have been published globally, with a significant proportion originating from scholars of the former Soviet Union. However, the non-publication of some studies internationally has constrained the overall progress of torsion field research [13].

Building on this research background and existing challenges, this paper attempts to derive a unified theoretical model of torsion fields and gravitational fields through precise modeling of vacuum scalar wave equations and particle propagation models, systematically elucidating their essential connotations, internal connections, and interaction mechanisms. The es-

tablishment of these new theoretical models not only refines the torsion field theoretical framework and addresses mainstream academic skepticism but may also provide novel analytical tools and implementation pathways for forward-looking topics such as anti-gravitational fields, wireless energy transmission, and future free energy. This holds significant theoretical value and application prospects for advancing gravitational theory innovation, new energy development, and the progress of related interdisciplinary fields.

2. The wave equations and particle propagation model of scalar waves

2.1. The wave equations of scalar waves

In a conductor medium, the total current law and Faraday's law of electromagnetic induction [13, 14] can be expressed as

$$\begin{aligned}\nabla\times\vec{B}/\mu\varepsilon &= \nabla\times\vec{B}_t/\mu\varepsilon+\nabla\times\vec{B}_\theta/\mu\varepsilon\\ &=\frac{\partial\vec{E}_t}{\partial t}+\frac{\vec{J}}{\varepsilon}\\ &=\frac{\partial\vec{E}_t}{\partial t}-(\nabla\times\vec{E})\vec{V}_e\\ &=\frac{\partial\vec{E}_t}{\partial t}-\vec{V}_{et}\frac{\rho}{\varepsilon}-(j\vec{k}\times\vec{E}_z)\,\vec{V}_{ez}\\ &=\frac{\partial\vec{E}_t}{\partial t}+\vec{E}_t\frac{\sigma}{\varepsilon}+\vec{E}_z\frac{\sigma}{\varepsilon}\\ &=\frac{\partial\vec{E}_t}{\partial t}+\frac{\vec{E}_t}{\tau_1}+\frac{\vec{E}_z}{\tau_1}\end{aligned}\tag{1}$$

$$\begin{aligned}\nabla\times\vec{E}&=\nabla\times\vec{E}_t+\nabla\times\vec{E}_z\\ &=-\frac{\partial\vec{B}}{\partial t}=-\frac{\partial\vec{B}_t}{\partial t}-\frac{\partial\vec{B}_\theta}{\partial t}\\ &=-\frac{\partial\vec{B}_t}{\partial t}-\frac{\vec{B}_\theta}{\tau_1}\end{aligned}\tag{2}$$

Here, $\vec{E}_t\,/\,\vec{B}_t$ represents the transverse electromagnetic (TEM) waves (specifically speaking, $\vec{E}_t$ is transverse electric field and $\vec{B}_t$ is transverse magnetic field), while $\vec{E}_z\,/\,\vec{B}_\theta$ represents the longitudinal electromagnetic waves, i.e. scalar waves (specifically speaking, $\vec{E}_z$ is scalar electric field and $\vec{B}_\theta$ is vortex magnetic field); $\vec{k}$ is the wave vector, $\vec{J}$ denotes the current density in the conductor; ε, μ, ρ and σ are the permittivity, permeability, free charge density, and conductivity of the conductor, respectively; $\vec{V}_e$ represents the velocity of the electric field (current) that generates the total electromagnetic waves in the conductor, $-\vec{V}_{et}$ represents the velocity of the electric field (current) that generates the TEM waves in the conductor, and $-\vec{V}_{ez}$ represents the velocity of the electric field (current) that generates the scalar waves in the conductor (depicted in Figure 1); τ_1 is the time decay constant of the vortex magnetic field $\vec{B}_\theta$ [14]. By splitting Equations (1) and (2) into two parts, namely the TEM wave and scalar wave components, we can derive that the total current law and Faraday's law of electromagnetic induction for the scalar wave in the conductor can be expressed as:

$$\nabla\times\vec{B}_\theta/\mu c=\frac{\partial\vec{E}_z}{\partial t}=\frac{\vec{E}_z}{\tau_1}=\frac{\sigma\vec{E}_z}{\varepsilon}\tag{3}$$

$$\nabla\times\vec{E}_z=-\frac{\partial\vec{B}_\theta}{\partial t}=-\frac{\vec{B}_\theta}{\tau_1}\tag{4}$$

As reported in [14], when two coherent light waves with a phase difference of π (termed as "source light waves") are superposed in a conductor, a pair of scalar waves $\vec{E}_z/\vec{B}_\theta$ will be generated. The wave equations are given by Equations (3) and (4), and their plane-wave solutions are expressed as Equations (5) and (6).

$$\vec{B}_\theta=\frac{E_{z0}}{V_B}\exp\left[j\left(\frac{\omega_p}{V_{ez}}z-\omega_p t\right)\right]\vec{e}_\theta\tag{5}$$

$$\vec{E}_z=E_{z0}\exp\left[j\left(\frac{\omega_p}{V_{ez}}z-\omega_p t\right)\right]\vec{e}_z\tag{6}$$

where

$$V_{ez}V_B=\frac{1}{\mu\varepsilon}\tag{7}$$

Moreover, with reference to Equations (5) and (6), the electromagnetic scalar potential φ and

the magnetic vector potential $\vec{A}_z$ of the scalar wave $\vec{E}_z/\vec{B}_\theta$ in the conductor can be written as:

$$\vec{A}_z = A_{z0} \exp\left[j\left(\frac{\omega_p}{V_{ez}} z - \omega_p t\right)\right] \vec{e}_z \tag{7.1}$$

$$\varphi = \varphi_0 \exp\left[j\left(\frac{\omega_p}{V_{ez}} z - \omega_p t\right)\right] \tag{7.2}$$

where they satisfy the following expression [15] shown as:

$$\varphi = A_z V_B \tag{7.3}$$

Here, τ_1 is the time decay constant of the vortex magnetic field $\vec{B}_\theta$ and also the wave period of the scalar wave $\vec{E}_z/\vec{B}_\theta$, ω_p is the frequency of $\vec{E}_z/\vec{B}_\theta$, V_{ez} represents both the magnitude of the velocity of the electric field (current) that generates $\vec{E}_z/\vec{B}_\theta$ and the phase velocity of them, while V_B is the phase velocity of the source light waves that gives rise to $\vec{E}_z/\vec{B}_\theta$ (see Figure 1). For a typical metal medium [16], with $\varepsilon \sim 10^{-11}$ F/m, $\mu \sim 10^{-6}$ H/m, $\sigma \sim 10^7$ S/m, taking $\omega = 10^{13}$ Hz $\ll \sigma/\varepsilon \sim 10^{17}$ Hz yields

$$V_B = \sqrt{\frac{2\omega}{\mu\sigma}} \sim 10^6 \text{ m/s}$$

and

$$V_{ez} \sim 10^{10} \text{ m/s} \gg V_B$$

Equations (5) and (6) unveil the electromagnetic induction law of the scalar wave $\vec{E}_z/\vec{B}_\theta$. That is to say, the scalar electric field $\vec{E}_z$ and the vortex magnetic field $\vec{B}_\theta$ can be mutually converted in a conductor and propagate forward with the same phase angle. We postulate that when the scalar waves $\vec{E}_z/\vec{B}_\theta$ transition from the conductor into the vacuum, the frequency ω_p remains unchanged, while the wave speed V_{ez} becomes the speed of light, i.e.,

$$V_{ez} = V_B = \sqrt{\frac{1}{\mu_0 \varepsilon_0}} = C \tag{7.4}$$

Figure 2 depicts the wave pattern of the scalar waves $\vec{E}_z/\vec{B}_\theta$ propagating in a vacuum as defined by Equations (5) and (6), indicating that they propagate along the positive z axis in a vacuum with the same phase angle and at the phase velocity C.

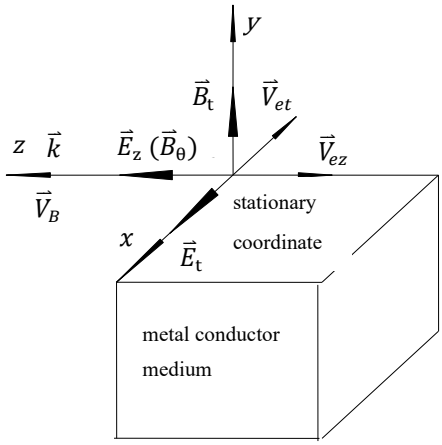

Figure 1: Electromagnetic fields in a continuous conductor.

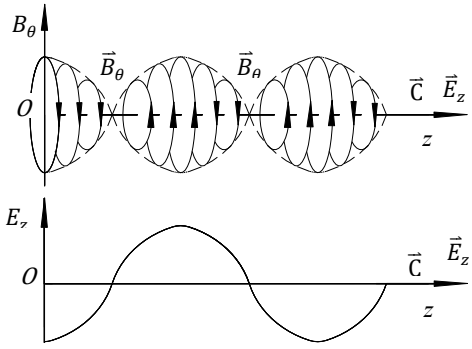

Figure 2: The propagation mode of $\vec{E}_z/\vec{B}_\theta$ in a vacuum.

2.2. The particle propagation model and motion equations of scalar waves

In accordance with [5], the particle propagation model of the vacuum scalar waves is depicted in Figure 3, which is composed of two left-handed neutrinos with a phase difference of π. Both of them have a spin velocity equal to the speed of light and perform a large left-handed helical orbital motion along the forward axis. The velocity in the z-direction, V_z, is also equal to the speed of light. Since neutrinos have mass, their tangential rotational velocity V_θ cannot ex-

ceed the speed of light [17]. Supposing that the mechanism by which the neutrino rotates around the core of the scalar waves at this moment is consistent with that of the ground-state electron rotating around the hydrogen atomic nucleus [18], we can derive that:

$$V_\theta = \frac{C}{137} \tag{8}$$

According to Gauss's law for electric fields [13], the divergence of the electric field within a conductor can be expressed as:

$$\begin{aligned} \nabla \times \vec{E} = \nabla \times \vec{E}_z = jkE_z = j\frac{\omega_p}{V_{ez}}E_z \\ = -j\frac{\rho\sigma E_z}{-\rho V_{ez}\sigma}\omega_p = -j\frac{\rho}{\sigma}\omega_p = \frac{\rho}{\epsilon} \end{aligned} \tag{9}$$

Here, k is the scalar wave vector. Based on Equation (9), the frequency ω_p of the scalar wave $\vec{E}_z/\vec{B}_\theta$ can be expressed as:

$$\omega_p = j\frac{\sigma}{\varepsilon} = \frac{j}{\tau_1} \sim 10^{17}\ \text{Hz} \tag{10}$$

Consequently, the energy ratio of the vacuum scalar wave $\vec{E}_z/\vec{B}_\theta$ to the source light waves that gives rise to them can be expressed as:

$$\frac{E_P}{E_T} = \frac{\hbar\omega_p}{\hbar\omega} = \frac{10^{17}}{10^{13}} = 10^4 \tag{10.1}$$

which implies that, apart from the energy E_T of the source light waves, $\vec{E}_z/\vec{B}_\theta$ must also draw a substantial amount of additional free energy from the zero-point vacuum field [6, 19]. Here, $\hbar$ is the Planck's constant. The mechanism through which the scalar wave $\vec{E}_z/\vec{B}_\theta$ obtains free energy is associated with the local spatial vortex motion generated by the vortex magnetic field $\vec{B}_\theta$. This vortex motion can extract zero-point vacuum energy via the coherent resonance interaction between the torsion field it generates and the zero-point vacuum energy field [6, 9].

Given that the scalar wave $\vec{E}_z/\vec{B}_\theta$ absorbs a large quantity of vacuum free energy, this energy, analogous to the local space-bending effect induced by a massive object (where space bending gives rise to a gravitational field), will exert a notable spatial vortex (distortion) effect on the internal space of the scalar-wave helix. This effect gives rise to a local spatial tangential vortex motion $V_{\theta 1}$ and a z-direction bending motion V_{z1} (depicted in Figure 4).

For the sake of model simplification, it is assumed that the speed V_{z1} of the local spatial z-direction bending motion generated by the scalar wave $\vec{E}_z/\vec{B}_\theta$ is significantly smaller than the local spatial tangential vortex motion $V_{\theta 1}$ generated concurrently, and the influence of the macroscopic expansion motion in the z-direction of space is neglected. Consequently, the motion equation of the propagation particle–neutrino of the vacuum scalar wave $\vec{E}_z/\vec{B}_\theta$ in vacuum can be formulated as:

$$\vec{V} = \vec{C} - \vec{V}_{\theta 1} = C\vec{e}_z - \frac{c}{137}\vec{e}_\theta - V_{\theta 1}\vec{e}_\theta \tag{10.2}$$

Here, $\vec{e}_\theta$ is the tangential unit vector and $\vec{e}_z$ is the unit vector in the z-direction.

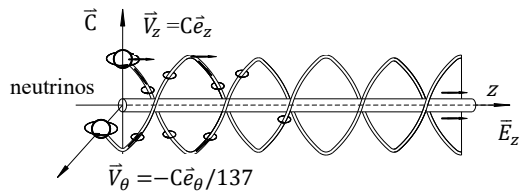

Figure 3: Particle propagation model of vacuum scalar waves.

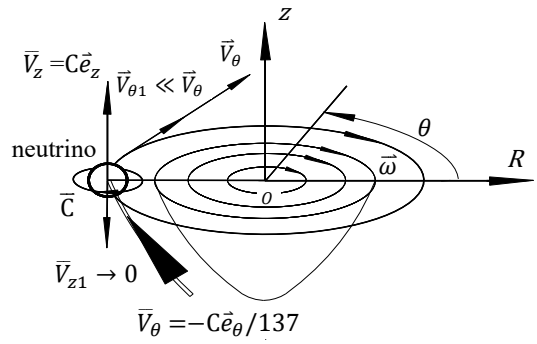

Figure 4: The helical motion of the neutrino around the core of the scalar waves.

3. The artificial torsion field and gravitational field generated by vacuum scalar waves

As depicted in Figure 5, within the vacuum space, we establish a region V of the field point P centered at point O on the Earth's surface. In the source region V' (centered at the fixed source point O' adjacent to field region V), there exist certain continuous, non-moving, and time-varying charges $\rho(\vec{r}',t)$ and a time-varying linear current source $\vec{J}_z(\vec{r}',t)$ that is excited by an external electromagnetic field. These sources generate the scalar waves $\vec{E}_z/\vec{B}_\theta$ within the region V. Furthermore, a cylindrical coordinate

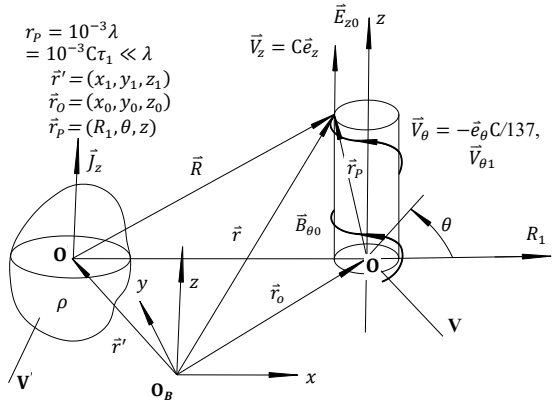

Figure 5: The helical motion of the neutrino around the core of the scalar waves.

system (R_1, θ, z) is established with an observer O_B as the origin on the Earth's surface. This coordinate system is employed to describe the propagation of the neutrino motion of $\vec{E}_z/\vec{B}_\theta$. When V' approaches zero and O_B coincides with O', the position vector $\vec{r}$ satisfies:

$$\begin{aligned} \vec{r} &= \vec{r}_P + \vec{r}_O \to \vec{R} \\ \frac{\partial R}{\partial t} &= \frac{\partial r}{\partial t} = \frac{\partial r_P}{\partial t} \\ &= \frac{\partial r_P}{\partial R_1}\frac{\partial R_1}{\partial t} + \frac{\partial r_P}{\partial \theta_1}\frac{\partial \theta_1}{\partial t} + \frac{\partial r_P}{\partial z}\frac{\partial z}{\partial t} \\ &= C - V_\theta - V_{\theta 1} \end{aligned} \tag{11}$$

Based on the relational formulas [20] between the scalar wave $\vec{E}_z/\vec{B}_\theta$ and the magnetic vector potential $\vec{A}_z$ the electromagnetic scalar potential φ, within region V, when the radial dimension $R_1 = 10^{-3}\lambda \sim 10^{-12}\,\mathrm{m} \ll \lambda \sim 10^{-9}\,\mathrm{m}$ and $V_{\theta 1} \ll V_\theta$, we can derive that:

$$\begin{aligned} \vec{B}_\theta &= \nabla \times \vec{A}_z \\ &= \frac{\mu_0}{4\pi}\int_{V'} -R^{-2}(\vec{e}_R \times \vec{J}_z)\, dV' \\ &= \vec{e}_R \times \frac{\mu_0}{4\pi}\int_{V'} -R^{-2}\vec{J}_z\, dV' \end{aligned} \tag{12}$$

$$\begin{aligned} \vec{E}_z &= -\nabla\varphi - \frac{\partial \vec{A}_z}{\partial t} \\ &= -j\frac{\omega_p V_B}{V_{ez}}A_z + j\omega_p A_z \approx j\omega_p A_z = -\frac{\partial \vec{A}_z}{\partial t} \\ &= \frac{\mu_0}{4\pi}\frac{\partial R}{\partial t}\int_{V'} -R^{-2}\vec{J}_z\, dV' \\ &= -(C - V_\theta - V_{\theta 1})\,\vec{e}_R \times \vec{B}_\theta \end{aligned} \tag{13}$$

where λ is the wavelength of $\vec{E}_z/\vec{B}_\theta$, μ_0 is the vacuum permeability and $\vec{e}_R$ is the radial unit vector.

Taking the derivative of Equation (12) gives that:

$$\frac{\partial \vec{E}_z}{\partial t} = a_\theta \vec{e}_R \times \vec{B}_\theta - \vec{e}_R \times \vec{B}_\theta \frac{C}{\tau_1} + \vec{e}_\theta \times \vec{B}_\theta \frac{V_\theta}{\tau_1}, \tag{14}$$

In Equation (14), assuming that C/τ_1 corresponds to the strong nuclear force field, and then V_θ/τ_1 is highly likely to represents the electromagnetic field, and a_θ equaling $\partial V_{\theta 1}/\partial t = V_{\theta 1}/\tau_1$ might represent the gravitational field. Equation (14) seemingly unifies the nuclear force, electromagnetic force, and gravitational field in form [17].

According to Equation (13), the conversion relationship between the scalar wave electromagnetic fields $\vec{E}_z/\vec{B}_\theta$ that generates the torsion field and the gravitational field can be expressed as:

$$\vec{E}_z = V_{\theta 1}\,\vec{e}_R \times \vec{B}_\theta \tag{15}$$

$$V_{\theta 1}^2\,\vec{B}_\theta = -V_{\theta 1}\,\vec{e}_R \times \vec{E}_z \tag{16}$$

Here, $E_z = -V_{\theta 1}B_\theta$, which indicates that the scalar waves $\vec{E}_z/\vec{B}_\theta$ that generate the torsion field and the gravitational field are out of

phase with π. By taking the derivative of Equation (15), the z-directional bending acceleration field of the local space, namely the gravitational field $\vec{a}_z$, generated by the local-space distortion motion induced by $\vec{B}_\theta/\vec{E}_z$ can be expressed as:

$$\vec{a}_z = a_\theta \vec{e}_z = \vec{e}_z \frac{V_{\theta 1}}{\tau_1} = -\frac{\vec{E}_z}{B_\theta \tau_1} = -\frac{1}{B_\theta}\frac{\partial \vec{E}_z}{\partial t} = -\frac{1}{B_\theta}\frac{\partial E_z}{\partial t}\vec{e}_z \tag{17}$$

when $\dfrac{\partial E_z}{\partial t} > 0$, that is, the linear electric field E_z increases,

$$\vec{a}_z = a_\theta \vec{e}_z = -\frac{1}{B_\theta}\frac{\partial E_z}{\partial t}\vec{e}_z = -\vec{e}_z \frac{V_{\theta 1}}{\tau_1} \tag{17.1}$$

when $\dfrac{\partial E_z}{\partial t} < 0$, that is, the linear electric field E_z decreases,

$$\vec{a}_z = a_\theta \vec{e}_z = -\frac{1}{B_\theta}\frac{\partial E_z}{\partial t}\vec{e}_z = \vec{e}_z \frac{V_{\theta 1}}{\tau_1} \tag{17.2}$$

Evidently, the expression of $\vec{a}_z$ generated by $\vec{B}_\theta/\vec{E}_z$ still adheres to Newton's laws of motion. Its direction is either the same as or opposite to the propagation direction of the scalar electric field $\vec{E}_z$ of the scalar wave, depending on the rate of change of E_z.

By taking the derivative of Equation (16), the spatial tangential distortion acceleration fields, that is, the torsion fields $\vec{a}_R$ and $\vec{a}_\theta$, generated by the local-space distortion motion induced by $\vec{B}_\theta/\vec{E}_z$ can be expressed as:

$$\vec{a}_R = a_\theta \vec{e}_R = -\vec{e}_R \frac{V_{\theta 1}}{\tau_1} = -\vec{e}_\theta \times \frac{\vec{E}_z}{B_\theta \tau_1} \tag{17.3}$$

$$\vec{a}_\theta = a_\theta \vec{e}_\theta = -\vec{e}_\theta \frac{V_{\theta 1}}{\tau_1} = -\vec{e}_R \times \frac{\vec{E}_z}{B_\theta \tau_1} \tag{17.4}$$

In conclusion, the magnitudes of the torsion field and gravitational field generated by the vacuum scalar wave are related to the variation period τ_1 and the electromagnetic conversion rate of the scalar-wave electromagnetic fields, that is, they are related to the tangential vortex motion velocity $V_{\theta 1}$ of the distortion motion generated by the scalar wave $\vec{B}_\theta/\vec{E}_z$ in the local space within their helix. Equations (17.1)–(17.4) suggest the following rules determining the generation of the torsion field and gravitational field by scalar wave vortex electromagnetic fields.

1. The expressions of the torsion field and gravitational field generated by the scalar wave $\vec{B}_\theta/\vec{E}_z$ still comply with Newton's laws of motion.
2. The direction of the gravitational field $\vec{a}_z$ is either the same as or opposite to the propagation direction of the linear scalar wave, depending on the rate of change of the linear electromagnetic field.
3. The direction of the torsion field $\vec{a}_R$ is as depicted in Figure 6, which is a helical centripetal acceleration field.
4. The torsion field $\vec{a}_\theta$ causes an object in the local space within the scalar-wave helix to rotate counterclockwise (viewed from the negative to the positive direction of z ($\vec{E}_z$), see Figure 6).

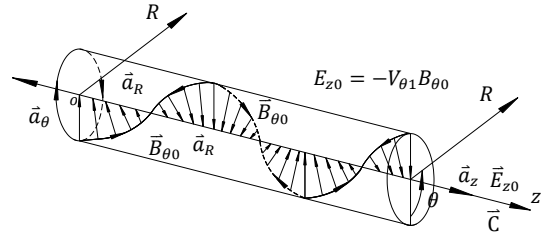

Figure 6: Artificial torsion field and gravitational field generated by vacuum scalar waves.

4. Qualitative experimental verifications

4.1. Rotation direction of the artificial torsion field

The working principle of the experimental apparatus for generating an artificial torsion field using the coils is depicted in Figure 7. Inside a

horizontally positioned vacuum chamber with a diameter of 10 cm, a small red polyethylene ball with a mass of 0.35 g is vertically suspended. The vacuum chamber is evacuated to preclude the rotation of the ball caused by the electrostatic motor effect and the ion-wind effect. Two

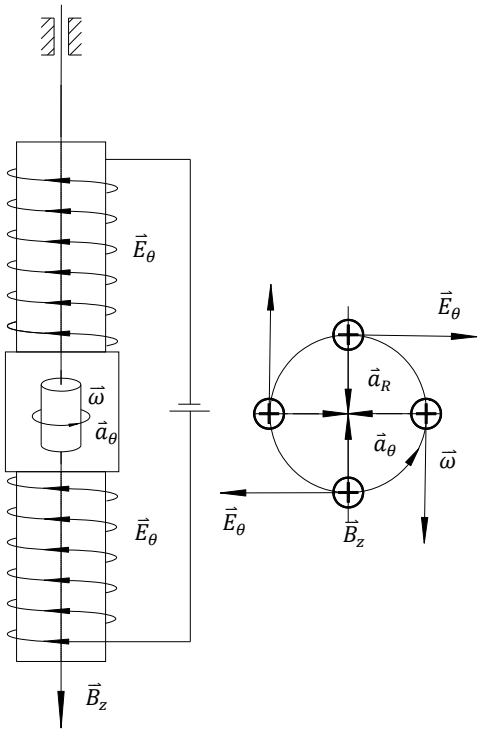

Figure 7: Schematic diagram of the working principle of the experimental setup for generating artificial torsion fields by coils.

coils wound with silicone-coated wires are installed at the top and bottom of the vacuum chamber respectively. For each coil, the number of turns $N = 30$, the radius r of the cross-section A is equal to 4 cm, and the length $l = 12$ cm. The coil wire is a copper wire with a diameter of 1.5 mm. These two coils are separated by the vacuum chamber. One end of each coil is connected to the positive and negative poles of a pulsed direct current source with a frequency of 3×10^4 Hz and a voltage of 10^5 V.

Since the electric field can readily penetrate the thick glass of the vacuum chamber, it is impossible to completely eliminate the polarization effect of the electric field. Nevertheless, in the specially designed coil structure of this experiment, the central axis of the coil coincides precisely with the central axis of the suspended polyethylene ball. The force resulting from the polarization effect acts along the direction parallel to the central axis, while the polyethylene ball rotates around the central axis of the coil. Consequently, the polarization effect has no impact on the rotation of the polyethylene ball.

At the instant when the current I is applied to the coils, if the manual switch-pressing time τ_1 is 0.3 s, the expression of the induced electromotive force ε_i is shown as follows [21]:

$$\frac{\varepsilon_i}{l} = dE_\theta = -\frac{NA}{l}\frac{dB_z}{dt} = -\frac{NA}{l}\frac{B_z}{\tau_1} \qquad (17.5)$$

Based on Equations (14) and (17.5), the artificial torsion field a_θ generated at the instant when the coil shown in Figure 7 is powered on can be expressed as:

$$a_\theta = \frac{dE_\theta/dt}{B_z} = -\frac{NA}{l}\frac{1}{\tau_1^2} = 1.396\,g \qquad (17.6)$$

Evidently, a_θ is now of the same order of magnitude as the gravitational field g on the Earth, and can exert a notable rotational effect on the polyethylene ball.

4.2. Artificial gravitational field generated by Michelson interferometer

In September 2025, Mr. Zhang and Dr. Huang's research team carried out an experiment on generating an artificial gravitational field using a vortex magnetic field with the aid of a Michelson interferometer. They set up the positive and negative electrodes of the Michelson interferometer with a distance l equaling 8 cm between them and a cross-sectional radius r_0 equaling 1.5 mm. A 50,000-volt pulsed direct current was applied. A light beam passed perpendicularly through the middle of the electrodes (as depicted in Figure 8). The manual on-off time of the circuit was set to 0.05 s. According to the theoretical prediction of Equation (17), at the instant when the circuit is switched on and off, if the vortex magnetic field

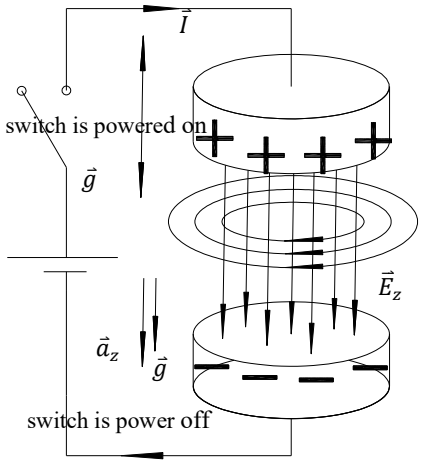

Figure 8: Schematic of the principle for the artificial gravity field experiment using a Michelson interferometer.

generates a gravitational field of sufficient magnitude, the degree of curvature of the local space near the electrodes will change. This change will alter the light path, thereby causing a variation in the width of the interference fringes of the Michelson interferometer. Based on the formula for the vortex-induced magnetic field B_θ generated by an approximately infinitely long straight wire [22] and the formula for the self-inductance coefficient L of an approximately infinitely long straight wire [21], the induced electromotive force ε_i caused by the rate of change of current dI/dt in the wire can be expressed as:

$$\begin{aligned}\varepsilon_i &= dE_z\, l \\ &= -L\frac{dI}{dt} = -\frac{\mu_0 l}{8\pi}\frac{dI}{dt} = -\frac{2\pi r_0}{\mu_0}\frac{\mu_0 l}{8\pi}\frac{dB_\theta}{dt}\end{aligned} \tag{17.7}$$

Based on Equations (17.7) and (17), the artificial gravitational field $\vec{a}_z$ generated by the Michelson interferometer depicted in Figure 8 can be expressed as:

$$\begin{aligned}a_z &= \frac{1}{B_\theta}\frac{\partial E_z}{\partial t} \\ &= \frac{E_z}{B_\theta \tau_1} = \frac{r_0}{4\tau_1^2} = 1.3\ \mathrm{m/s^2} = 0.13\, g\end{aligned} \tag{17.8}$$

It is evident that the artificial gravitational field $\vec{a}_z$ generated by the Michelson interferometer at this instant exerts a notable influence on the gravitational field g on the Earth. As depicted in Figure 8, at the moment when the switch is closed, the linear electric field $\vec{E}_z$ commences to increase from zero. At this time, $dE_z/dt > 0$ and $dB_\theta/dt < 0$. Based on Equation (17.2), the direction of the artificial gravitational field $\vec{a}_z$ generated by B_θ is opposite to that of $\vec{E}_z$. That is to say, $\vec{a}_z$ weakens the gravitational field, reducing the degree of bending in the z-direction within the space of the vortex magnetic field B_θ. This leads to a decrease in the optical path and a narrowing of the width of the light interference fringes.

When the switch is opened, the linear electric field $\vec{E}_z$ begins to decrease, with $dE_z/dt < 0$, and $dB_\theta/dt > 0$. According to Equation (17.1), the direction of the artificial gravitational field $\vec{a}_z$ generated by B_θ is the same as that of $\vec{E}_z$. In other words, $\vec{a}_z$ enhances the gravitational field, increasing the degree of bending in the z-direction within the space of the vortex magnetic field B_θ, augmenting the optical path, and widening the width of the light interference fringes. The experimental results are presented

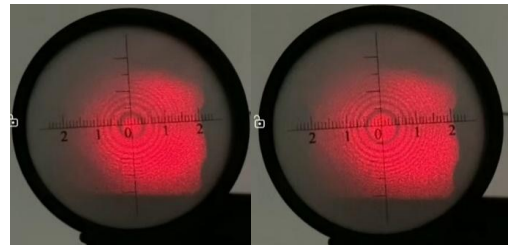

(a) switch is turned off (b) switch is turned on

Figure 9: Influence of the artificial gravitational field on the interference fringes of the Michelson interferometer.

in Figure 9. It was observed that at the moment of circuit on-off, the width of the bright-dark interference fringes exhibited a distinct change. Moreover, the trend of this change was in full accordance with the theoretical predictions of Equations (17.1) and (17.2). Since this experiment did not involve electrode discharge, it completely circumvented the influence of medium alterations on the optical path [23]. Consequently, it provides conclusive evidence for the existence of scalar waves and the fact that vortex electromagnetic fields can generate artificial gravitational fields.

5. Discussion

5.1. The Gravitational field generated by TEM waves could be neglected

Employing the same analytical approach, the formula for the gravitational field generated by TEM waves (taking light waves as an illustrative example) can be derived as:

$$\frac{\partial \vec{E}_t}{\partial t} = -\vec{a}_t \times \vec{B}_t \tag{18}$$

where $\vec{a}_t = -V_{\theta 1}\,\omega \vec{e}_t$. Considering $\omega_p \approx 10^{31}\,\text{Hz} \gg \omega = 10^{13}\,\text{Hz}$, by comparing with the gravitational-field formula of scalar waves, it can be deduced that $a_t \ll a_\theta$. This suggests that scalar waves are primarily responsible for generating artificial gravitational and torsion fields, while the contribution of TEM waves to them is negligible. From an alternative perspective, the energy of TEM waves $\vec{E}_t/\vec{B}_t$ is insufficient to induce local spatial vortex motion. Consequently, they are unable to generate artificial torsion field and gravitational field.

5.2. Scalar waves and future new energy sources

The energy ratio between vacuum scalar waves and source light waves is 10000 : 1. This implies that scalar waves must extract a vast amount of additional free energy from the zero-point vacuum field. The mechanism by which scalar waves obtain free energy is related to the local spatial vortex motion induced by the scalar wave vortex electromagnetic field. This vortex electromagnetic field can extract zero-point vacuum energy through the entangled interaction between the torsion field they generate and the zero-point vacuum energy field.

When two source light waves superpose in a vacuum, the electromagnetic fields seemingly vanish. However, the magnetic vector potential $\vec{A}_\theta$ persists and gives rise to:

$$\vec{E}_\theta = -\frac{\partial \vec{A}_\theta}{\partial t} = \sqrt{2}\,C B_0\,\vec{e}_\theta \exp\left[j\left(\frac{\omega_p}{C}z - \omega_p t\right)\right] \tag{19}$$

and

$$\vec{B}_z = \nabla \times \vec{A}_\theta = \sqrt{2}\,B_0\,\vec{e}_z \exp\left[j\left(\frac{\omega_p}{C}z - \omega_p t\right)\right] \tag{20}$$

which is referred to as a "vacuum artificial free-energy field" with substantial energy [19].

Schnabl and Meyl's experiments [24, 25] have validated the mechanism of scalar-wave absorption of free energy. He discovered that scalar waves possess unique energy characteristics. Specifically, they can increase the content of adenosine triphosphate (ATP) in the mitochondria of morning glories by 40%, thereby extending the flowering period by nearly 10%.

We can utilize this principle to obtain copious amounts of free energy. In the future, this free energy may potentially supplant fossil fuels and electrical energy, emerging as the primary energy source. Additionally, this free energy can be disseminated to numerous households via the wireless energy-transmission mode of vacuum scalar waves through wireless networks. This presents an extremely promising prospect for the application of new energy sources.

5.3. A possible unified field equation

As reported in [15, 19], when two coherent "source light waves" with a phase difference of π and a frequency of ω are superposed in vacuum, a pair of scalar waves $\vec{E}_\theta/\vec{B}_z$ will be generated. The frequency ω_P of $\vec{E}_\theta/\vec{B}_z$ can be expressed as:

$$\omega_P = j\,\frac{1}{\tau_2} = j\,\frac{\omega^2 \varepsilon_0}{\sigma_0} = 1.129 \times 10^{31}\,\text{Hz} \tag{21}$$

Here, τ_2 is the period of fluctuation of scalar waves $\vec{E}_\theta/\vec{B}_z$, σ_0 is the vacuum conductivity, ε_0 is the vacuum permittivity.

Based on the relational formulas between the scalar waves $\vec{B}_z/\vec{E}_\theta$ and the magnetic vector potential $\vec{A}_\theta$ the electromagnetic scalar potential φ_θ [19], and adopting the same analytical approach as that in Section 3 of this paper, we can

derive that:

$$\begin{aligned}\vec{B}_z &= \nabla \times \vec{A}_\theta \\ &= \frac{\mu_0}{4\pi}\int_{V'} -R^{-2}(\vec{e}_R \times \vec{J}_\theta)\, dV' \\ &= \vec{e}_R \times \frac{\mu_0}{4\pi}\int_{V'} -R^{-2}\vec{J}_\theta\, dV'\end{aligned} \tag{22}$$

$$\begin{aligned}\vec{E}_\theta &= -\nabla\varphi_\theta - \frac{\partial \vec{A}_\theta}{\partial t} = \frac{\mu_0}{4\pi}\frac{\partial R}{\partial t}\int_{V'} -R^{-2}\vec{J}_\theta\, dV' \\ &= (C - V_\theta - V_{\theta 1})\,\vec{e}_R \times \vec{B}_z\end{aligned} \tag{23}$$

Differentiating Equation (23) yields that:

$$\begin{aligned}\frac{\partial \vec{E}_\theta}{\partial t} &= -\vec{a}_R \times \vec{B}_z \\ &\quad + \frac{C}{\tau_2}\,\vec{e}_R \times \vec{B}_z + \frac{C}{\tau_2}\,\vec{e}_\theta \times \vec{B}_z \\ &\quad - \frac{V_\theta}{\tau_2}\,\vec{e}_R \times \vec{B}_z \\ &\quad - \frac{V_\theta}{\tau_2}\,\vec{e}_\theta \times \vec{B}_z - \vec{a}_\theta \times \vec{B}_z\end{aligned} \tag{24}$$

In Equation (24), $C/\tau_2 \sim 10^{39}\,\mathrm{m/s^2}$ corresponds to the strong nuclear force field generated by the linear motion of particles at the speed of light $C\vec{e}_z$ in the z-direction during scalar wave propagation, $V_\theta/\tau_2 \sim 10^{37}\,\mathrm{m/s^2}$ undoubtedly represents the electromagnetic field generated by its tangential light-speed rotational motion $V_\theta\vec{e}_\theta$, $a_R, a_\theta = V_{\theta 1}/\tau_2 \sim 10\,\mathrm{m/s^2}$ represent the torsion field and gravitational field generated by the scalar waves' vortex motion. Equation (24), based on the wave equations of the vacuum scalar waves $\vec{B}_z/\vec{E}_\theta$ and the neutrino particle-propagation model, seemingly unifies the nuclear force, electromagnetic force, and torsion field force (gravitational force) in form. Perhaps, at the scalar wave level, the unified field equation that we have been painstakingly pursuing may indeed be so simple.

6. Conclusion

On the basis of the vacuum scalar wave equation and particle model, we have derived the theoretical models of the torsion field and gravitational field generated by the scalar-wave vortex electromagnetic field. Through experiments, we have verified the direction of the gravitational field generated by the vortex magnetic field, thereby comprehensively uncovering the essence of the torsion field and gravitational field.

As scalar waves draw in a substantial amount of vacuum free energy, this energy gives rise to a notable vortex effect within the internal space of the scalar-wave helix. The acceleration field that induces tangential distortion motion in the local space due to this vortex effect constitutes the torsion field, while the acceleration field that causes z-direction bending motion in the local space is the gravitational field.

The magnitudes of the torsion field and gravitational field generated by vacuum scalar waves are associated with the variation period and electromagnetic conversion rate of the scalar-wave electromagnetic field. In other words, they are related to the velocity of this spatial vortex motion. When an electric current gives rise to a magnetic field, the direction of the gravitational field generated by the scalar wave is either opposite to or the same as the direction of the linear electromagnetic field of the scalar electromagnetic field, which depends on the temporal rate of change of the vortex electromagnetic field.

Acknowledgements

I would like to thank my wife, Ms. Xue Jingwen for her hard family work and support for my creation of this thesis.

Competing Interests

Authors declare that they have no competing interests.

Data and Materials Availability

All data are available in the main text or the supplementary materials.

Ethical Approval Statement

The study did not require ethical approval.

References

[1] N. A. Kozyrev. On the possibility of experimental investigation of the properties of time. *Time in science and philosophy*, pp. 111-132, 1971.

[2] H. Hayasaka and S. Takeuchi. Anomalous weight reduction on a gyroscope's right rotations around the vertical axis on the earth. *Physical review letters*, 63(25):2701, 1989. DOI: 10.1103/PhysRevLett.63.2701.

[3] A. E. Akimov and G. I. Shipov. Torsion fields and their experimental manifestations. *Journal of New Energy*, 2:67-84, 1997.

[4] É. Cartan. Sur les variétés à connexion affine et la théorie de la relativité généralisée (première partie). *Annales scientifiques de l'École normale supérieure*, 40:325-412, 1923. DOI: 10.24033/asens.751.

[5] G. I. Shipov. A Theory of Physical Vacuum and Torsion Fields. *Akademiya Nauk SSSR*, Priroda, 11:3-14, 1993.

[6] X. L. Jiang, J. Z. Lei, and L. J. Han. Torsion field and tapping the zero-point energy in an electrochemical system. *Journal of New Energy*, 4(2):93-95, 1999.

[7] J. Xingliu, L. Zhijian, W. Xiongwei, and H. Lijun. Transient vortex dynamics and anomalous nuclear phenomena in nonequilibrium system. *Nuclear Physics Review*, 21, 2004.

[8] S. C. Lee, X. G. Cai, and W. C. Liang. The Physical Nature of Crystalline Qi Field—Torison Field. *Buddhism and Science*, 2:59-72, 2016.

[9] J. Z. Jiang and X. Y. Chen. Wave Equations and Particle Propagation Model of TCM (Traditional Chinese Medicine) Qi and Its Interaction with Water. *J. Evolutionary Medicine*, 12(6):92-9, 2024.

[10] D. Reed. Excitation and extraction of vacuum energy via EM-torsion field coupling-theoretical model. *Journal of New Energy*, 3(2):130-140, 1998.

[11] K. Meyl. Skalarwellen: Theorie und Experimente zur Feldumwandlung. *Villingen-Schwenningen: INDEL*, 1996/1998.

[12] F. W. Hehl, P. von der Heyde, G. D. Kerlick, and J. M. Nester. General relativity with spin and torsion: Foundations and prospects. *Reviews of Modern Physics*, 48(3):393, 1976. DOI: 10.1103/RevModPhys.48.393.

[13] Y. M. Zhang and B. Y. Qi. Electromagnetism (2nd ed.). *Beijing: Science Press*, ISBN: 978-7-03-017997-5, 2007.

[14] J. Jianzhong. A mode of electromagnetic wave propagation based on the inter-induction of scalar electric field and vortex magnetic field. *Journal of Environmental Science and Engineering B*, 13:134–143, 2024. DOI: 10.17265/2162-5263/2024.04.002.

[15] J. Z. Jiang and Y. F. Wang. Analysis of the Electromagnetic Characteristics and the Mechanism Underlying Bio-Medical Function of Longitudinal Electromagnetic (LEM) Waves. *Journal of Energy and Power Engineering*, 12(10):31–49, 2024. DOI: 10.4236/jpee.2024.1210002.

[16] K., Huang. Solid State Physics (Revised by Han R. Q.). *Beijing, China: Higher Education Press*, 1988. ISBN 10: 7040010259 / ISBN 13: 9787040010251.

[17] J. Jiang and X. Chen. An Analysis about the Origin and Essence of Mass Based on Particle-Propagating Model and Wave Equations of Scalar Waves. *Journal of Environmental Science and Engineering B*, 14:65–75, 2025. DOI: 10.17265/2162-5263/2025.02.003.

[18] N. Bohr. On the Constitution of Atoms and Molecules. *Philosophical Magazine*, 26:1-25, 1913. DOI: 10.1080/14786441308634955.

[19] J. Jianzhong and Y. Wang. The magnetic longitudinal (P-) wave's propagation and energy models underlying the mechanisms of its capacity to absorb free energy. *Journal of Power and Energy Engineering*, 12(7), 2024. DOI: 10.4236/jpee.2024.127003.

[20] Y. Aharonov and D. Bohm. Significance of electromagnetic potentials in the quantum theory. *Physical Review*, 115(3):485–491, 1959. DOI: 10.1103/PhysRev.115.485.

[21] F. Chen and X. Jin. College Physics (Daxue Wulixue). *Beijing: Science Press*, ISBN: 978-7-03-024834-3, 2009.

[22] S. H. Guo. Electrodynamics. *China Higher Education Press*, pp. 121-158, 2008.

[23] C. M. Glenn. Experimental Spacetime Distortion: Generating Gravitational Waves in the Laboratory. *European Journal of Engineering and Technology Research*, 10(2):39-48, 2025. DOI: 10.24018/ejeng.2025.10.2.3246.

[24] H. Schnabl and K. Meyl. Longitudinal magnetic waves trigger higher ATP-levels and extend the aging process of plants. *Biol Eng Med*, 3:1-4, 2018. DOI: 10.15761/BEM.1000156.

[25] H. Schnabl and K. Meyl. Anti-Aging by longitudinal magnetic waves: A new approach by modulating ATP-Levels. *Biol. Eng. Med*, 4:1-5, 2019. DOI: 10.15761/BEM.1000175.

About Authors

Jiang Jian-zhong Doctor of Engineering, Associate Professor, School of Mechanical Engineering, Jiangnan University, China. Research Interests: Food Machinery; Scalar Wave Torsion Field Theory; Energy Medicine. He can be contacted at email: 8043000163@jiangnan.edu.cn.